

BRIDGE: A Direct-tree Hybrid N -body Algorithm for Fully Self-consistent Simulations of Star Clusters and their Parent Galaxies

Michiko FUJII

*Department of Astronomy, Graduate School of Science, The University of Tokyo, 7-3-1 Hongo, Bunkyo, Tokyo 113-0033
fujii@astron.s.u-tokyo.ac.jp*

Masaki IWASAWA, Yoko FUNATO

*Department of General System Studies, College of Arts and Sciences, The University of Tokyo, 3-8-1 Komaba, Meguro, Tokyo
153-8902*

*iwasawa@margaux.astron.s.u-tokyo.ac.jp, funato@artcompsci.org
and*

Junichiro MAKINO

*Division of Theoretical Astronomy, National Astronomical Observatory of Japan, 2-21-1 Osawa, Mitaka, Tokyo, 181-8588
makino@cfca.jp*

(Received 2000 December 31; accepted 2001 January 1)

Abstract

We developed a new direct-tree hybrid N -body algorithm for fully self-consistent N -body simulations of star clusters in their parent galaxies. In such simulations, star clusters need high accuracy, while galaxies need a fast scheme because of the large number of the particles required to model it. In our new algorithm, the internal motion of the star cluster is calculated accurately using the direct Hermite scheme with individual timesteps and all other motions are calculated using the tree code with second-order leapfrog integrator. The direct and tree schemes are combined using an extension of the mixed variable symplectic (MVS) scheme. Thus, the Hamiltonian corresponding to everything other than the internal motion of the star cluster is integrated with the leapfrog, which is symplectic. Using this algorithm, we performed fully self-consistent N -body simulations of star clusters in their parent galaxy. The internal and orbital evolutions of the star cluster agreed well with those obtained using the direct scheme. We also performed fully self-consistent N -body simulation for large- N models ($N = 2 \times 10^6$). In this case, the calculation speed was seven times faster than what would be if the direct scheme was used.

Key words: stellar dynamics — methods: numerical, n-body simulations — galaxies: star clusters

1. Introduction

Very young and massive stars have been found in the central parsec of the Galaxy (Krabbe et al. 1995; Paumard et al. 2001; Paumard et al. 2006). These stars are very young (< 10 Myr) (Paumard et al. 2001; Ghez 2003) and lie on two disks (Paumard et al. 2006). The disks rotate around the central black hole (BH) and are at a large angle with each other. One disk rotates clockwise in projection, the other counterclockwise, although the existence of the counterclockwise disk is controversial (Lu et al. 2006). These disks are coeval to within 1 Myr.

However, in situ formation of these stars seems unlikely since the strong tidal field of the central super massive black hole prevents the gas density from reaching the Roche value high enough for star formation through self gravity. To solve this problem, two possibilities have been suggested: (1) star formation in situ in a dense gaseous disk around Sgr A*, or (2) infall of a young star cluster.

The disk model was proposed by Levin & Beloborodov (2003). A dense gaseous disk is formed, when a infalling molecular cloud is tidally disrupted by the central BH. If the density exceeds $M/2\pi R^3$ at radius R , where M is the mass of the central BH, the disk becomes unstable with

respect to its own gravity and starts to fragment. The fragments collapse and star formation occurs. However, this model is problematic. Observations have shown that two disks are at large angles with respect to each other and these stars on the disks formed almost at the same time. In this in situ formation scenario, two disks at large angles must have existed within 1 Myr, unless one disk changed its orientation through, for example, external perturbation.

The star cluster inspiral model was proposed by Gerhard (2001). A star cluster is formed at a distance of tens of parsecs from the Galactic center (GC) and spiraled into the GC due to dynamical friction before being disrupted by the tidal field of the central black hole. In the central 30 pc, two young dense star clusters, the Arches and Quintuplet clusters, are observed (Nagata et al. 1995; Figer 2004). This model can naturally explain the existence of two stellar disks. Numerical simulations of this model have been performed (Portegies Zwart et al. 2003, hereafter PZ03; Kim & Morris 2003; Gürkan & Rasio 2005). These simulations showed that it took too long for the star cluster to sink to the central parsec unless it was very massive ($> 10^6 M_\odot$) or the initial position of the star cluster is very near from the GC (2pc or less).

In these simulations (PZ03; Gürkan & Rasio 2005), the dynamical friction from the Galaxy on the star cluster was calculated analytically using the dynamical friction formula (Chandrasekhar 1943). However, it is not clear whether this analytical treatment of the orbital evolution is correct in the case of star clusters. For rigid objects, the orbital evolutions obtained using the analytical treatment agree well with those obtained using N -body simulations, if $\ln \Lambda$ is determined correctly taking into account the distance from the galactic center and the size of the object (Hashimoto et al. 2003; Spinnato et al. 2003). However, our fully self-consistent N -body simulation of a satellite galaxy within its parent galaxy showed that the orbital decay of the satellite is much faster than those calculated analytically using the dynamical friction formula, even if the correct value of $\ln \Lambda$ is used (Fujii et al. 2006). This difference is caused by the enhancement of the dynamical friction by particles escaped from the satellite. In the case of star clusters, the same enhancement should occur. Thus, a fully self-consistent N -body simulation is necessary to obtain correct results for the orbital evolution of star clusters.

Such a fully self-consistent N -body simulation has not been performed because it was impossible with existing numerical methods. There are two classes of numerical methods for N -body simulations. One is the direct summation, suitable for collisional systems, and the other is schemes for collisionless systems such as tree, SCF, and particle-mesh schemes. Neither of them can handle such multi-scale systems like star clusters within galaxies.

The direct summation is the simplest and the most accurate way to calculate forces; for a particle we calculate $N - 1$ inter-particle forces and sum them up. Thus the cost to integrate all N particles is $O(N^2)$. The combination of direct summation, Hermite integrator and individual timesteps is widely used. It can achieve very high accuracy. Hence, this method is used for simulations of collisional systems such as star clusters, planetary formation, and galactic nuclei with central BHs. However, we cannot use this method for galaxies because its cost is too high.

The tree algorithm (Barnes & Hut 1986; Makino 2004) is an approximate algorithm to calculate forces. It can achieve $O(N \log N)$ scaling. This method is often used with 2nd-order leapfrog integrator. This method is very powerful for systems which need many particles and in which particles have similar timescales, such as galaxies or large scale structures. Tree code is difficult to combine with individual timesteps and high order integration schemes. Therefore, the tree algorithm is not suitable for collisional systems. Other schemes for collisionless systems have similar proper times.

Fully self-consistent N -body simulations of star clusters which orbit in their parent galaxy require (1) accurate time integration for star clusters and (2) fast time integration for the parent galaxy. Neither of direct or tree (or collisionless) methods, however, can satisfy these requirements. This is the reason why fully self-consistent N -body simulations of star clusters within galaxies have

never been performed.

A way to solve this problem is an algorithm based on tree code with individual timesteps (Hernquist & Katz 1989; McMillan & Aarseth 1993). This approach, however, has problems with the accuracies and/or the costs. Furthermore, it is difficult to use GRAPE with such a method.

We developed a new algorithm which is an extension of the mixed variable symplectic (MVS) method developed for long-term integration of planetary systems (Wisdom & Holman 1991; Kinoshita et al. 1991). In our new scheme, star clusters are integrated using direct summation and Hermite scheme with individual timesteps, while galaxies are integrated using the tree code and leapfrog scheme with shared timestep. We combine them by embedding direct scheme into the tree code. Using this new algorithm, we have made it possible to perform fully self-consistent N -body simulations of star clusters which orbit in their parent galaxies with very accurate time integration for star clusters and fast time integration for the parent galaxy.

We describe our new algorithm in section 3 after a description of the MVS method in section 2. In section 4, we show the results of test simulations and performance of our new algorithm. We summarize in section 5.

2. The Mixed Variable Symplectic Method

The MVS integrator were introduced by Wisdom & Holman (1991) and by Kinoshita, Yoshida, & Nakai (1991). It is now widely used for long-term integrations of planetary systems. In the case of planetary systems, their Hamiltonian can be divided into Kepler motions and interaction between planets. The MVS integrator suppresses the error of the motion due to the numerical integration of the solar potential since it integrates the Kepler motions analytically.

Let us first describe briefly a symplectic integrator, the leapfrog scheme. The Hamilton equation is rewritten in terms of a Poisson bracket operator as

$$\frac{df}{dt} = \{f, H\}, \quad (1)$$

where f is a function of t . If we introduce a differential operator D_H defined as $D_H f := \{f, H\}$, the formal solution of equation (1) is written as

$$f(t) = e^{tD_H} f(0). \quad (2)$$

An integration algorithm can be thought of as an approximate expression of this operator.

As an example, we describe a second-order leapfrog integrator. The Hamiltonian for an N -body system is written as

$$H = \sum_i^N \frac{p_i^2}{2m_i} - \sum_{i<j}^N \frac{Gm_i m_j}{r_{ij}}. \quad (3)$$

If we define

$$H_A = - \sum_{i < j}^N \frac{G m_i m_j}{r_{ij}} \quad (4)$$

$$H_B = \sum_i^N \frac{p_i^2}{2m_i}, \quad (5)$$

then we can express the the formal solution, the time evolution from t to $t + \Delta t$, as

$$f(t + \Delta t) = e^{\Delta t(A+B)} f(t), \quad (6)$$

where $A := D_{H_A}$ and $B := D_{H_B}$. This operator can be rewritten by the Taylor series as

$$e^{\Delta t(A+B)} = \prod_{i=1}^k e^{a_i \Delta t A} e^{b_i \Delta t B} + O(\Delta t^{n+1}), \quad (7)$$

where (a_i, b_i) ($i = 1, 2, \dots, k$) is a set of real numbers and n is a given integer, which corresponds to the order of integrator. By neglecting the $O(\Delta t^{n+1})$ then, we obtain a mapping from $f(t)$ to $f'(t + \Delta t)$ as

$$f'(t + \Delta t) = \prod_{i=1}^k e^{a_i \Delta t A} e^{b_i \Delta t B} f(t). \quad (8)$$

This mapping is symplectic because it is just a product of symplectic mappings. This is an n -th order symplectic integrator. We can achieve $n = 2$ with $k = 2$, with the choice of the coefficients $a_1 = a_2 = 1/2$ and $b_1 = 1, b_2 = 0$. Now, equation (7) is reduced to

$$e^{\Delta t(A+B)} = e^{\frac{1}{2} \Delta t A} e^{\Delta t B} e^{\frac{1}{2} \Delta t A} + O(\Delta t^3). \quad (9)$$

Therefore the time evolution is expressed as

$$f'(t + \Delta t) = e^{\frac{1}{2} \Delta t A} e^{\Delta t B} e^{\frac{1}{2} \Delta t A} f(t). \quad (10)$$

This is the second-order leapfrog scheme, which is rewritten as

$$\mathbf{v}_{\frac{1}{2}} = \mathbf{v}_0 + \frac{1}{2} \Delta t \mathbf{a}_0, \quad (11)$$

$$\mathbf{x}_1 = \mathbf{x}_0 + \Delta t \mathbf{v}_{\frac{1}{2}}, \quad (12)$$

$$\mathbf{v}_1 = \mathbf{v}_0 + \frac{1}{2} \Delta t \mathbf{a}_1, \quad (13)$$

where subscripts, 0, $\frac{1}{2}$, 1, correspond to values at $t, t + \frac{1}{2} \Delta t, t + \Delta t$, respectively.

The procedure of leapfrog scheme is as follows.

1. Calculate the acceleration at a time, t , and update the velocity [eq. (11)].
2. Update positions using new velocity $\mathbf{v}_{\frac{1}{2}}$ [eq. (12)].
3. Calculate the acceleration at $t + \Delta t$ using the new positions, \mathbf{x}_1 , and update velocity [eq. (13)].
4. Repeat 1-3.

Now, we explain an MVS integrator. The Hamiltonian for a planetary system can be expressed as

$$H = H_{\text{Kep}} + H_{\text{Int}}, \quad (14)$$

where H_{Kep} is the kinetic energy plus solar potential and H_{Int} is the interaction energy between planets. If we define

$$H_A = H_{\text{Int}}, \quad H_B = H_{\text{Kep}}, \quad (15)$$

equation (10) becomes

$$f'(t + \Delta t) = e^{\frac{1}{2} \Delta t I} e^{\Delta t K} e^{\frac{1}{2} \Delta t I} f(t). \quad (16)$$

Here $I := D_{H_{\text{Int}}}$ and $K := D_{H_{\text{Kep}}}$. Note that $e^{\Delta t K}$ generates motions of planets along unperturbed Kepler orbits, while $e^{\Delta t I}$ generates changes of momenta due to planet-planet interactions. This changes of momenta are called “velocity kicks.”

The difference from the usual leapfrog integrator is that $e^{\Delta t K}$ is given analytically by Kepler motion. Therefore the MVS method is expressed as

$$\mathbf{v}'_{\frac{1}{2}} = \mathbf{v}_0 + \frac{1}{2} \Delta t \mathbf{a}_{\text{Int},0}, \quad (17)$$

$$\mathbf{x}_0 \rightarrow (\text{Kepler motion}) \rightarrow \mathbf{x}_1, \quad (18)$$

$$\mathbf{v}_{\frac{1}{2}} \rightarrow (\text{Kepler motion}) \rightarrow \mathbf{v}'_{\frac{1}{2}}, \quad (19)$$

$$\mathbf{v}_1 = \mathbf{v}'_{\frac{1}{2}} + \frac{1}{2} \Delta t \mathbf{a}_{\text{Int},1}. \quad (20)$$

The integration proceeds as follows:

1. Calculate the accelerations of planets due to gravitational interactions between planets, $\mathbf{a}_{\text{Int},0}$, at time t and change velocities by giving the velocity kicks [eq.(17)].
2. Update the positions and the velocities by Δt along its osculating Kepler orbit analytically [eq.(18) and (19)].
3. Calculate $\mathbf{a}_{\text{Int},0}$ at $t + \Delta t$ and change velocities by giving the velocity kicks [eq.(20)].
4. Repeat 1-3.

MVS is a very powerful algorithm for long-term integration of planetary systems. In general, the integration errors are $O(\Delta t^n)$, where n is the order of the integrator. With a MVS integrator, if H_{Int} is $O(\epsilon)$ of H_{Kep} , the integration errors are only $O(\epsilon \Delta t^n)$. This ϵ is of the order of the planetary mass in the unit of solar mass and usually is very small. As a result, the error become much smaller than that of usual symplectic methods.

3. The New Hybrid Scheme

Now we consider simulations of systems consisting of a star cluster and its parent galaxy. For such a simulation, our new scheme should provide:

1. high accuracy for star clusters
2. fast integrator for galaxies
3. fully self-consistent treatment of the total system.

To achieve these goals, we constructed a new scheme which is a combination of the direct and the tree scheme. In our new scheme, the internal interactions of star clusters are calculated with high accuracy using the direct and Hermite scheme, while all other interactions (galaxy-galaxy, galaxy-star cluster) are calculated with the tree algorithm. We combine these two methods by extending the idea of the MVS.

In the MVS scheme, the Hamiltonian is divided into the kinetic energy plus solar potential and the interaction energy between planets. In our hybrid scheme, we separate the Hamiltonian as

$$H = H_\alpha + H_\beta, \quad (21)$$

$$H_\alpha = - \sum_{i < j}^{N_G} \frac{G m_{G,i} m_{G,j}}{r_{ij}} - \sum_{i=1}^{N_G} \sum_{j=1}^{N_{SC}} \frac{G m_{G,i} m_{SC,j}}{r_{ij}}, \quad (22)$$

$$H_\beta = \sum_{i=1}^{N_G} \frac{p_{G,i}^2}{2m_{G,i}} + \sum_{i=1}^{N_{SC}} \frac{p_{SC,i}^2}{2m_{SC,i}} - \sum_{i < j}^{N_{SC}} \frac{G m_{SC,i} m_{SC,j}}{r_{ij}}, \quad (23)$$

where N_G and N_{SC} are the number of the galaxy particles star cluster particles, respectively, and H_α is the potential energy of the gravitational interactions between galaxy particles and between galaxy particles and star cluster particles, while H_β is the kinetic energy of all particles and the potential energy of star cluster particles. Using the replacement $H_A = H_\alpha$ and $H_B = H_\beta$, we obtain the time evolution as

$$f'(t + \Delta t) = e^{\frac{1}{2}\Delta t \alpha} e^{\Delta t \beta} e^{\frac{1}{2}\Delta t \alpha} f(t), \quad (24)$$

where $\alpha = D_{H_\alpha}$, $\beta = D_{H_\beta}$.

In our scheme, we integrate star cluster particles and galaxy particles in different ways. Let us first discuss star cluster particles. They are integrated in a way similar to the MVS. The Keplerian in the MVS corresponds to the second and third terms in equation (23). Unlike the MVS, however, we cannot solve the Hamiltonian analytically. Hence, we replace an analytical solution (Kepler motion) in the MVS by a solution calculated by a higher-order integrator (e.g. the fourth-order Hermite integrator with individual timesteps).

Thus, the integrator for star clusters is written as

$$\mathbf{v}'_{SC,0} = \mathbf{v}_{SC,0} + \frac{1}{2} \Delta t \mathbf{a}_{\{G \rightarrow SC,0\}}, \quad (25)$$

$$\mathbf{x}_{SC,0} \rightarrow (\text{Hermite scheme}) \rightarrow \mathbf{x}_{SC,1}, \quad (26)$$

$$\mathbf{v}'_{SC,0} \rightarrow (\text{Hermite scheme}) \rightarrow \mathbf{v}'_{SC,1}, \quad (27)$$

$$\mathbf{v}_{SC,1} = \mathbf{v}'_{SC,1} + \frac{1}{2} \Delta t \mathbf{a}_{\{G \rightarrow SC,1\}}, \quad (28)$$

where subscripts, SC and G, stand for the star cluster and the galaxy, subscripts, 0, $\frac{1}{2}$, and 1, indicate times t_0 , $t_{\frac{1}{2}} = t_0 + \frac{1}{2}\Delta t$, and $t_1 = t_0 + \Delta t$, respectively, and $\mathbf{v}'_{SC,\frac{1}{2}}$ represent a new velocity at $t_{\frac{1}{2}}$, which have been integrated using the Hermite scheme.

For galaxies, we use the leapfrog integrator expressed as

$$\mathbf{v}_{G,\frac{1}{2}} = \mathbf{v}_{G,0} + \frac{1}{2} \Delta t \mathbf{a}_{\{\text{All} \rightarrow G,0\}}, \quad (29)$$

$$\mathbf{x}_{G,1} = \mathbf{x}_{G,0} + \Delta t \mathbf{v}_{G,\frac{1}{2}}, \quad (30)$$

$$\mathbf{v}_{G,1} = \mathbf{v}_{G,\frac{1}{2}} + \frac{1}{2} \Delta t \mathbf{a}_{\{\text{All} \rightarrow G,1\}}, \quad (31)$$

where $\mathbf{a}_{\{\text{All} \rightarrow G\}}$ denotes the acceleration due to gravitational forces from all particles (including star cluster particles) to the galaxy particle. The galaxy particles have

longer timescale than that of particles in the star cluster. Therefore, we adopt a second-order leapfrog integrator with shared timestep and tree algorithm. This scheme is less accurate than fourth-order Hermite scheme, but much faster and is symplectic.

We call our new scheme “the Bridge scheme” (Bridge is for Realistic Interactions in Dense Galactic Environment). The procedure of the Bridge scheme is summarized in figure 1 and as follows:

1. Make a tree at t_0 and calculate the accelerations from all particles on galaxy particles, $\mathbf{a}_{\{\text{All} \rightarrow G,0\}}$, and from galaxy particles on star cluster particles, $\mathbf{a}_{\{G \rightarrow SC,0\}}$, using the tree.
2. **Star cluster**: give a velocity kick [eq. (25)].
Galaxy: update velocity [eq. (29)].
3. **Star cluster**: integrate positions and the velocities from t_0 to t_1 using Hermite scheme with individual timesteps [eq. (26) and (27)].
Galaxy: Update position with leapfrog scheme [eq. (30)].
4. Make a new tree at t_1 and calculate the accelerations from all particles on galaxy particles, $\mathbf{a}_{\{\text{All} \rightarrow G,1\}}$, and from galaxy particles on star cluster particles, $\mathbf{a}_{\{G \rightarrow SC,1\}}$.
5. **Star cluster**: give a velocity kick [eq. (28)].
Galaxy: update velocity [eq. (31)].

As shown in equations (25) and (29), the forces on particles of galaxies and those on particles of star clusters are calculated differently. The former is from all particles, while the latter is from particles in the galaxy only. Therefore, we assigned two values of mass to each tree node. (We used center-of-mass approximation to forces from tree nodes.) One is total mass of all particles under the node, and the other is the mass of galaxy particles. To calculate forces on galaxy particles, we use the mass of all particles, and for star cluster particles we use the mass of galaxy particles.

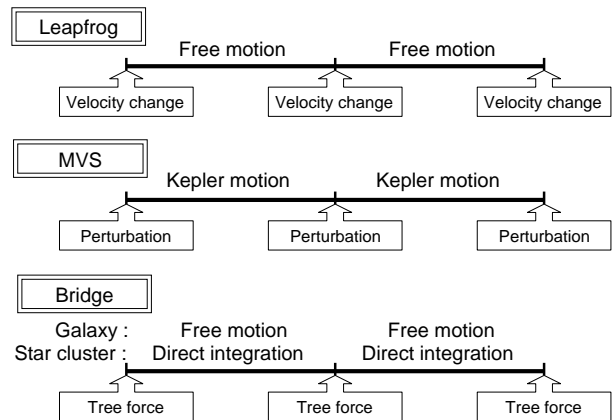


Fig. 1. Procedure of the Bridge scheme.

4. Accuracy and Performance

4.1. Comparison with Direct Scheme for Small- N Model

As a test of the Bridge scheme, we performed a fully self-consistent N -body simulation of a star cluster within a galaxy and compared the results with those obtained with the fourth-order Hermite scheme. In this section, we describe the results and the performance of the Bridge scheme.

We adopted a King model with the non-dimensional central potential $W_0 = 9$ as the model of the parent galaxy and with $W_0 = 7$ as that of the star cluster. The system of units is the Heggie unit (Heggie & Mathieu 1986), where the gravitational constant G is 1 and the mass and the binding energy of the parent galaxy are 1 and 0.25, respectively. The initial position of the star cluster is at distance 2.5 from the center of the parent galaxy and the initial velocity is 0.65. Both the galaxy and the star cluster are expressed as a self-consistent N -body models. The number of particles of the parent galaxy, N_G , is 10^5 and that of the star cluster, N_{SC} , is 2×10^3 . In table 1, we summarize the model parameters and initial conditions. If we assume the total mass of the star cluster $M_{SC} = 10^5 M_\odot$ and the unit length is 10 pc, the total mass of the Galaxy $M_G = 10^7 M_\odot$ and the unit time and velocity are 0.15 Myr and 66 km s $^{-1}$, respectively. These values would correspond to the central region of a galaxy somewhat smaller than our galaxy.

The potential is softened using the usual Plummer softening. The softening length for the gravitational interactions between star cluster particles is $\epsilon_{SC} = 2.0 \times 10^{-4} = 0.1 \times 4/N_{SC}$, and that between others (i.e. between galaxy particles and for galaxy particles and star cluster particles) is $\epsilon_G = 6.25 \times 10^{-3}$.

We used the opening angle $\theta = 0.75$ with the center-of-mass (dipole-accurate) approximation. The maximum group size for GRAPE calculation (Makino 1991) is 8192. For the leapfrog integrator, we adopted the stepsizes of $\Delta t = 1/128$ and $1/256$. The maximum timestep for the Hermite scheme with individual timesteps is equal to the timestep of the tree. All particles synchronize at each timestep for tree. Within these steps, star cluster particles are integrated the Hermite scheme with individual timesteps (Makino & Aarseth 1992). For the timestep criterion, we adopted the standard formula, which is given in Makino & Aarseth (1992). These parameters are summarized in table 2.

The simulations are performed on GRAPE-6 (Makino et al. 2003) for runs Direct 1 and 2, GRAPE-6A (Fukushige et al. 2005) for runs Bridge 1 and 2. We summarize them in table 3. Total energy was conserved to better than 0.06% when $\Delta t = 1/256$, 0.2% $\Delta t = 1/128$ with the Bridge scheme, and 0.006% with the Hermite scheme.

To compare the results, we followed the time evolution of the position, bound mass, core radius, and core density of the star cluster. The bound mass and orbit are calculated in the same way as in Fujii et al. (2006). We defined the core radius and the core density using the formula

proposed by Casertano & Hut (1985).

Table 1. Model Parameters of Testmodel

Parameters	Galaxy	Star cluster
Galactic halo	King 9	King 7
Total mass	1.0	0.01
Binding energy	0.25	2.5×10^{-4}
Half-mass radius	9.8×10^{-1}	8.1×10^{-2}
N	10^5	2×10^3
Initial position	(2.5, 0, 0)	
Initial velocity	(0, 0.65, 0)	

Table 2. Parameters for N -body Simulation

Parameters	Value
ϵ_G	6.25×10^{-3}
ϵ_{SC}	2.0×10^{-4}
θ	0.75
n_{crit}	8192
Δt	1/128, 1/256

Figures 2 and 3 show the evolution of the distance from the galactic center and the bound mass of the star cluster. Figures 4 and 5 show the core radius and the core density of the star cluster. These results show that the Bridge scheme works very well. The difference between the results of the Hermite scheme and that of the Bridge scheme is smaller than run-to-run variations in each method.

Figures 4 and 5 show that core collapse occurs at $T = 150 - 180$. Core collapse occurs at

$$t_{cc} \simeq ct_{rh}, \quad (32)$$

where t_{rh} is the star cluster's half-mass relaxation time (Spitzer & Hart 1971),

$$t_{rh} = 0.14 \frac{r_h^{3/2} N_{SC}}{(GM_{SC})^{1/2} \ln \Lambda}. \quad (33)$$

Here r_h , N_{SC} , and M_{SC} are the half-mass radius, the number of particles, and the mass of the star cluster. We adopted the Coulomb logarithm $\ln \Lambda \simeq \ln(0.1N_{SC})$. In isolated star cluster in which all stars has the same mass, $c \simeq 15$ (Cohn 1980). From these equations, the core collapse time of our cluster is calculated as $t_{cc} \simeq 180$. This value is consistent with the results of our simulation. Note that in our model we used the scaling of $M_G = 4E_G = 1$.

The total energy error of the system in Bridge 2 run is shown in Figure 6. The total energy is conserved very

Table 3. Runs

Runs	methods	seed	stepsize	run time (h)
Direct 1	direct	1	1/256	34
Direct 2	direct	2	1/256	34
Bridge 1	hybrid	1	1/128	10
Bridge 2	hybrid	2	1/256	19

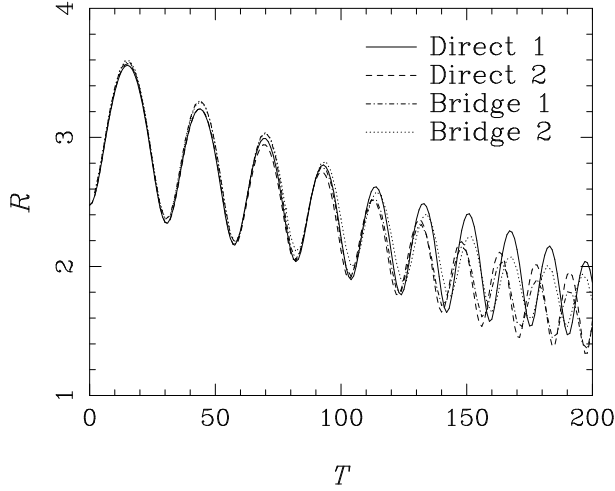


Fig. 2. Distance of the star cluster from the GC plotted as a function of time. Solid and dashed curves show the results of the runs in which all particles calculated with the direct (Hermite) scheme. Dashed-dotted and dotted curves show those with the Bridge scheme.

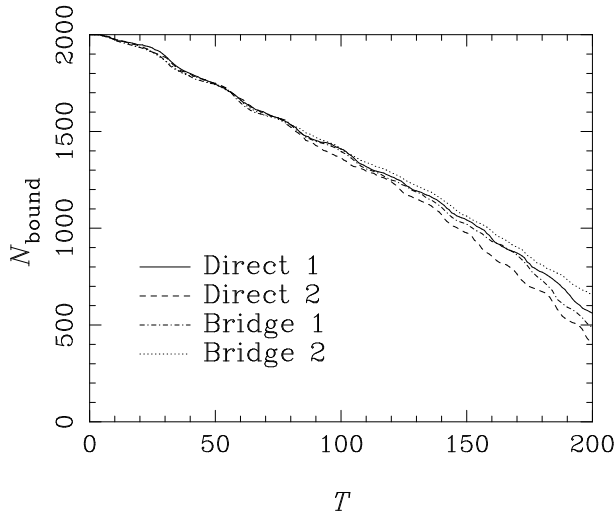


Fig. 3. Bound mass of the star cluster plotted as a function of time. Curves have the same meanings as in figure 2.

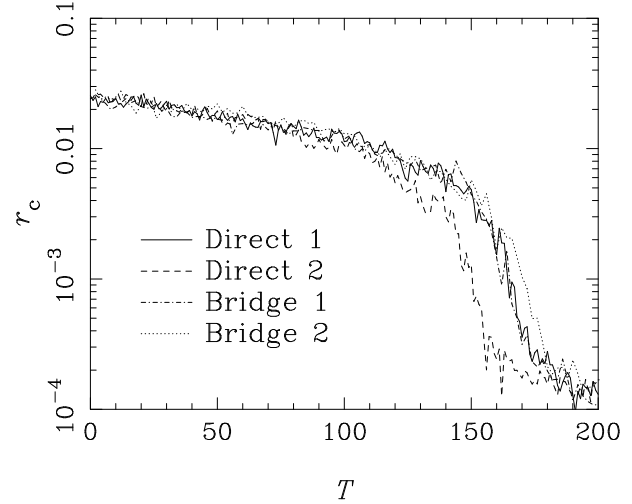


Fig. 4. Core radius, r_c , plotted as a function of time. Curves have the same meanings as in figure 2.

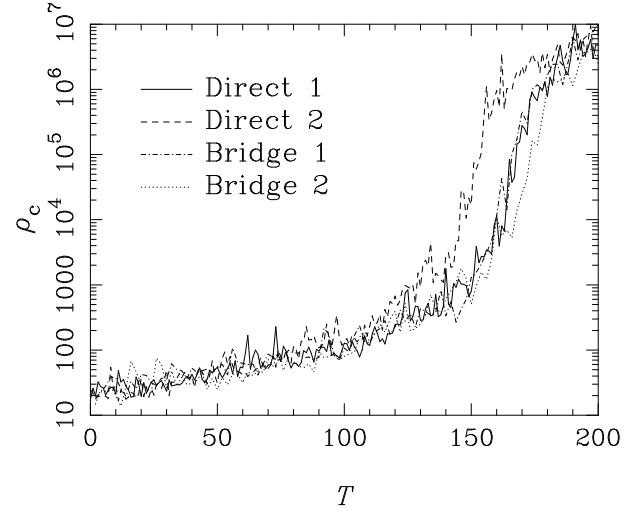


Fig. 5. Core density, ρ_c , as a function of time. Curves have the same meanings as in figure 2.

well. The total energy error depends on the parameters for tree, Δt and θ . This is because most of the energy error is generated in the parent galaxy, which is much larger than the star cluster and has much larger energy.

To see whether the internal energy of the star cluster is conserved or not, we measured the energy error of the internal motion of the star cluster within each step, Δt . The cumulative error of each step is shown in Figure 6. Note that we plot the energy error of the star cluster relative to the internal energy of the star cluster, which is 0.1 % of the total energy of the system. Although the error become larger after core collapse occurred, it is conserved well.

The distributions of the CPU time in runs with $\Delta t = 1/128$ and $\Delta t = 1/256$ are shown in table 4. In these simulations, the cost of the tree part was much larger than that of the direct part. The CPU time of the tree part is

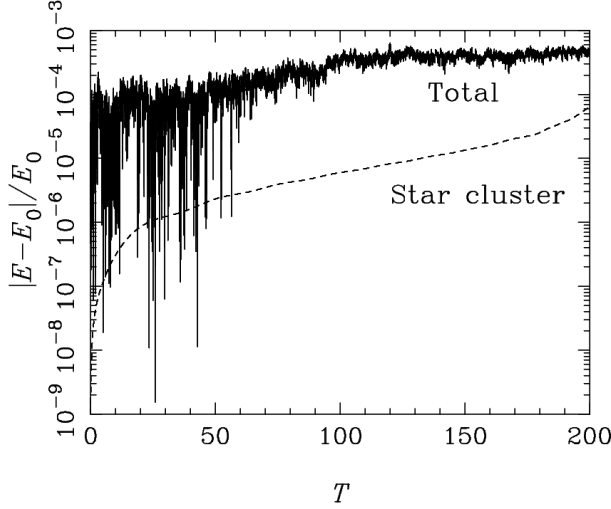


Fig. 6. The energy error of the system, for the hybrid run with $\Delta t = 1/256$ (Run Bridge 2). Full curve shows the total energy error of the system and dashed curve shows the cumulative energy error of the star cluster.

almost constant throughout the simulation. In contrast, the cost of the direct part increased after $T \simeq 140$, because the core density become higher.

Table 4. Distribution of the CPU Time of our Simulations

Section of Code	Percentage of CPU Time (%)	
	$\Delta t = 1/128$	$\Delta t = 1/256$
Tree	87.2	91.2
Direct	10.7	6.6
The others	2.1	2.2

4.2. Large- N Models

We performed simulations of large- N models. The number of particles is sufficiently large for simulations of star clusters near the GC ($N_G = 2 \times 10^6$, $N_{SC} = 65,536$). The model of the galaxy represents the central region of the Galaxy from ~ 1 to several pc from the GC. For the star cluster, we followed the model used in Portegies Zwart et al. (2003). They modeled the Arches and Quintuplet star clusters. The core radius of our model, r_{core} , is 0.087 pc. Using this model, we performed two simulations, in which the star cluster has circular and eccentric orbits, respectively. In table 4.2, we summarize the model parameters.

We performed N -body simulations using the Bridge code. For the tree part, we used the opening angle $\theta = 0.75$ with the center-of-mass (dipole-accurate) approximation. The maximum group size for a GRAPE calculation (Makino 1991) is 8192. The stepsize of leapfrog integrator is $\Delta t = 1/512$ (Heggie unit). The potential is softened using Plummer softening. The softening length for gravitational interactions between star cluster particles, ϵ_{SC} , is 1.0×10^{-5} pc and that for others, ϵ_G , is 3.9×10^{-2} pc. We stopped the simulations at $T = 0.75(\text{Myr}) = 5(\text{unit time})$. These parameters are summarized in table 6. After the

core collapse, the structures of the star clusters are not expressed correctly in our simulations because we use a softened potential for stars.

We used GRAPE-6 (Makino et al. 2003) for force calculation. The total energy was conserved better than 5×10^{-5} for the circular orbit (figure 9) and 8×10^{-5} for the eccentric orbit (figure 10) throughout the simulations.

Table 6. Parameters for N -body Simulation

Parameters	Value
ϵ_G	3.9×10^{-2} (pc)
ϵ_{SC}	1.0×10^{-5} (pc)
Δt (Heggie unit)	2.9×10^{-4} (Myr) 1/512
θ	0.75
n_{crit}	8192

Table 7. Initial Conditions

Simulation	Initial position (pc)	Initial velocity (km s^{-1})
Circular	2	130
Eccentric	5	72

Figure 7 show the snapshots from the run in which the orbit of the star cluster is eccentric. Figure 8 shows the time evolution of the distance from the GC, bound mass, and core radius of the star clusters. In both simulations, core collapse occurs at 0.5 - 0.6 Myr. We obtained the core collapse time, $t_{\text{cc}} = 0.51$ Myr, from equation (32) and (33), where the half-mass radius of the star cluster, $r_h = 0.13$ (pc). We adopted $c = 0.20$, which is suggested by (Portegies Zwart & McMillan 2002). The core collapse time of our simulations is consistent with the results of the previous studies.

Figure 9 and 10 show the total energy error of the system and the internal energy error of the star clusters. The internal energy errors are cumulative as in small- N models. The energies conserve very well.

The total CPU times and the distributions of the CPU time are shown in table 8. The total CPU time was about 40 hours. The direct part consumes about half of the CPU time.

4.3. Performance Model of the Hybrid Scheme

We analyzed the CPU time of each part in detail. Figure 11 shows the CPU time per 4 steps for each part for the run with circular orbit. Simulation time is represented using the Heggie unit. We used the parent galaxy to define the Heggie unit, i.e., $M_G = 4E_G = 1$. The unit time in the Heggie unit corresponds to 0.15 Myr. Hereafter we use the Heggie unit for time to discuss the performance of the hybrid scheme. The CPU time of the tree part is almost constant throughout the simulation. In contrast, the cost of the direct part gradually decreases and suddenly increase after $T \simeq 3.5$.

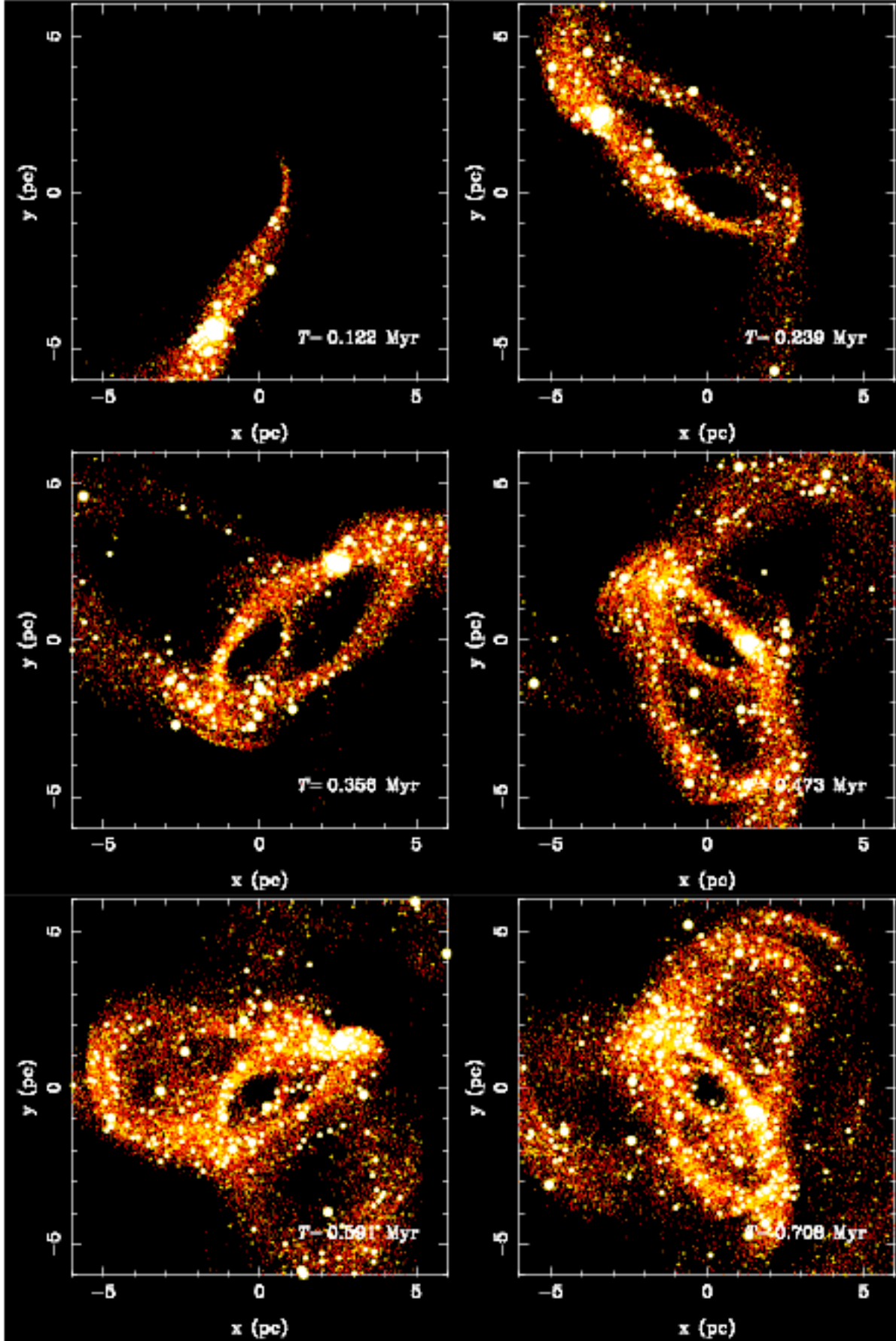
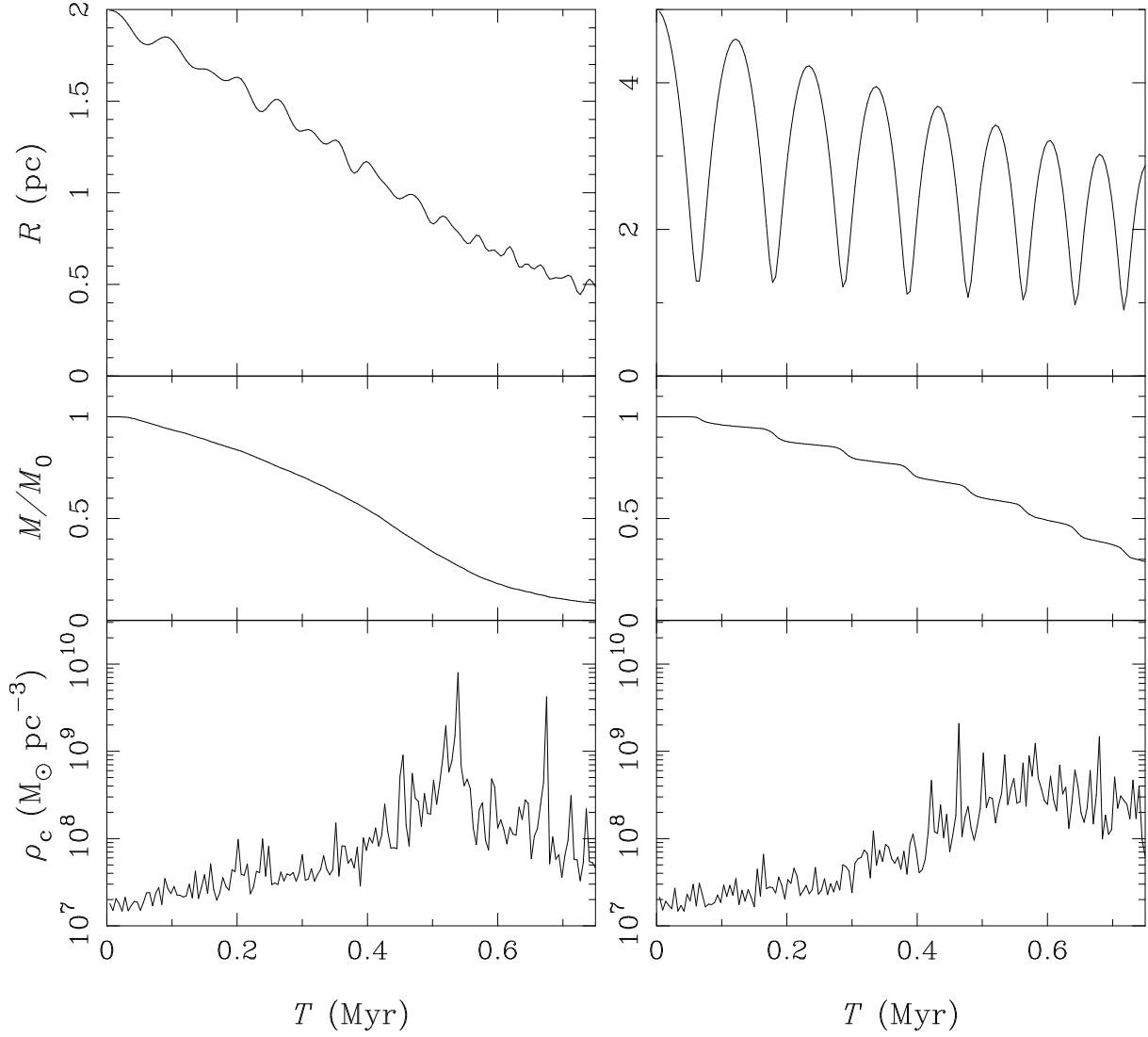


Fig. 7. Snapshots of the star clusters projected onto $x-y$ plane. The orbit of the star cluster is eccentric.

Table 5. Models

	King W_0	N	$M(M_\odot)$	r_c (pc)	r_t (pc)
The Galaxy	10	2×10^6	8.0×10^7	0.66	120
Star cluster	3	65536	7.9×10^4	0.087	0.47

**Fig. 8.** The distance from the GC (top), bound mass (middle), and core radius (bottom) of the star clusters plotted as a function of time. The orbits of the star clusters are circular in the left panels and eccentric in the right panels.**Table 8.** CPU percentage for the test models

Section of Code	CPU Time (sec)		Percentage of CPU Time (%)	
	Circular	Eccentric	Circular	Eccentric
Tree	5.6×10^4	6.3×10^4	42.3	45.3
Direct	7.5×10^4	7.5×10^4	56.9	53.6
The others	1.1×10^3	1.4×10^3	0.8	1.0
Total	$1.3 \times 10^5 \sim 37(h)$	$1.4 \times 10^5 \sim 39(h)$	100.0	99.9

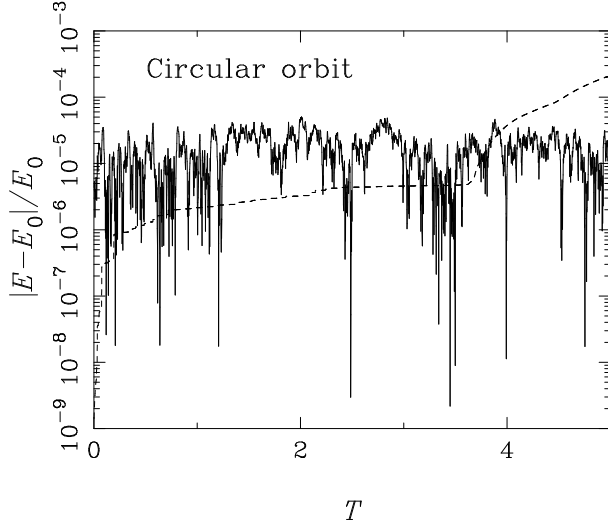


Fig. 9. Same as figure 6, but for large- N model with circular orbit.

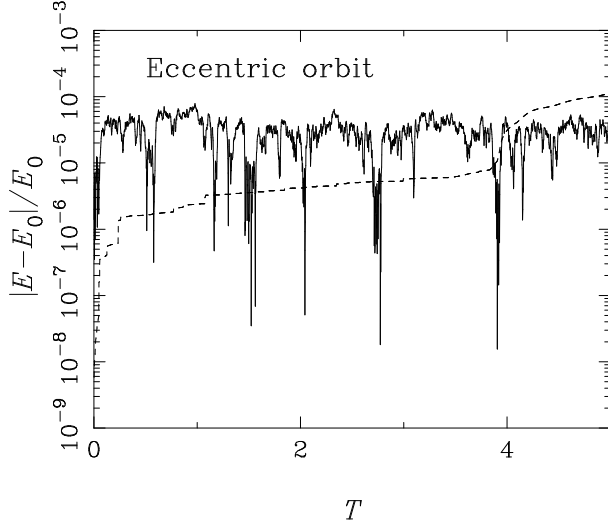


Fig. 10. Same as figure 6, but for large- N model with eccentric orbit.

As shown in figure 13, the CPU time of the direct part is proportional to the number of the steps for the Hermite scheme, n_{step} . Figure 12 shows the time evolution of the average number of timesteps per particle, n_{step} . It gradually decrease until $T = 3$, and stays nearly constant. In figure 13, CPU time suddenly increases starting at $T = 3.6$. This time corresponds to the time of core collapse, and after that the internal dynamics of the star cluster is not correctly followed because of the finite softening. In the discussions below, we consider the behavior of the CPU time before core collapse.

From these results, we can construct the performance model of the Bridge code. The total CPU time for a step, Δt , can be written by the number of the tree particles, N_{tree} , that of the direct particles, N_{direct} , and that of steps for Hermite scheme per step, n_{step} . The cost of tree is

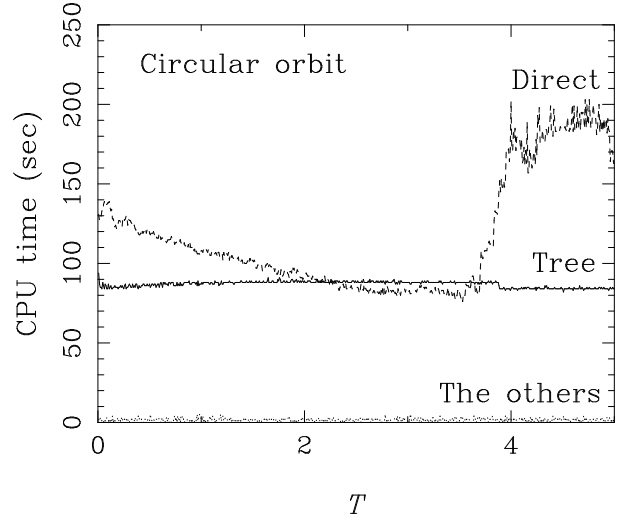


Fig. 11. CPU time of the direct and tree parts per 4 steps ($\Delta t = 1/128$) for the circular orbit. The solid, dashed, and dotted curves show the CPU time of tree, direct, and the others parts, respectively.

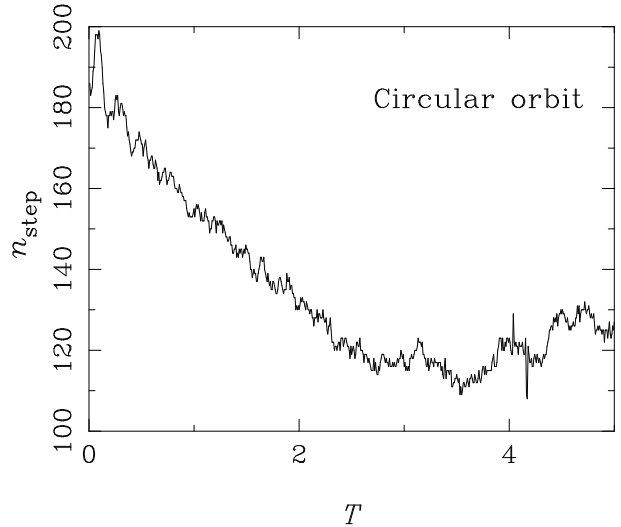


Fig. 12. The number of steps of the direct part per particle per 4 steps (1/128 unit time) for the circular orbit.

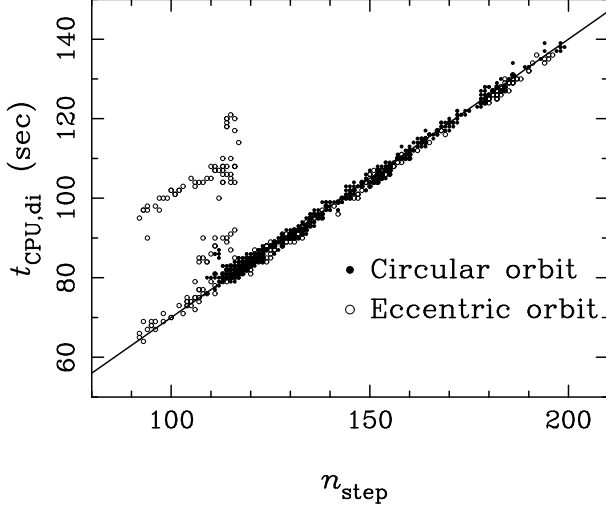


Fig. 13. The CPU time of the direct part per 4 steps (1/128 unit time) before $T = 3.6$. Filled circle and open circle show the results of the circular orbit and eccentric orbit. Solid line shows the model of equation (34).

proportional to $N_{\text{tree}} \log N_{\text{tree}} \sim N_{\text{tree}}$. The CPU time of the direct part depends on N_{tree} and n_{step} . The cost of force calculation is proportional to N_{direct}^2 and the other costs are proportional to N_{direct} . Therefore, the total CPU time per Δt is given by

$$T_{\text{CPU}} = \alpha N_{\text{tree}} + (\beta N_{\text{direct}} + \gamma N_{\text{direct}}^2) n_{\text{step}}, \quad (34)$$

where α , β , and γ are constants. Here, α is almost constant through a simulation, but depends on θ . The value of γ is determined by the performance of GRAPE. Makino et al. (2003) shows that the calculation time on GRAPE per interaction per particle is expressed as

$$T_{\text{GRAPE}} = \frac{1}{9 \times 10^7 n_{\text{pipes}}} \text{ (sec)}, \quad (35)$$

where n_{pipes} is the total number of pipelines. With GRAPE-6A $n_{\text{pipes}} = 24$, with GRAPE6 $n_{\text{pipes}} = 192$. Hence, we estimated $\gamma = 4.6 \times 10^{-10}$ (sec), for GRAPE-6A, $\gamma = 5.8 \times 10^{-11}$ (sec) for GRAPE-6. From the results of our runs, we estimated the values of the constants, $\alpha = 1.2 \times 10^{-5}$ (sec) for $\theta = 0.75$ and $\beta = 6.9 \times 10^{-6}$ (sec).

The number of particles that we need for fully self-consistent N -body star cluster simulation is $N_G \sim 2 \times 10^6$ for a galaxy and $N_{\text{SC}} \sim 6.5 \times 10^4$ for a star cluster. In this case, the total CPU time for the Bridge scheme is estimated as 1.2×10^5 sec ~ 34 hours for a simulation with $\Delta t = 1/512$ and 5 unit time integration on GRAPE-6. Here we used $n_{\text{step}} = 33$ from the results of our simulations. The actual time for such a simulation was 37 - 39 hours (see table 8). So our model predicts the CPU time with ~ 20 % accuracy.

We can also estimate that for the Hermite scheme. The CPU time of the Hermite scheme, or the direct scheme, can be estimated using the second and third terms of equation (34), where we used $n_{\text{step}} = 770$ per unit time. Therefore, the total CPU time is estimated as about 260

hours per 5 unit times on GRAPE-6 for $N = 2 \times 10^6$. It's about seven times longer than that for the Bridge scheme.

5. Summary and Discussion

5.1. Summary

We have developed a fast and accurate algorithm, “the Bridge scheme,” for fully self-consistent N -body simulations of a star cluster moving in its parent galaxy, where both are modeled as N -body systems. The Bridge scheme is a hybrid of the tree and direct schemes and is based on an extension of MVS. We performed self-consistent N -body simulations of a star cluster in a galaxy and compared the results with the Bridge scheme and that with the direct scheme (the Hermite scheme). They agreed each other very well and the energy error was sufficiently small. We also showed that we can perform a full N -body simulation of a star cluster and a galaxy system with $N_{\text{SC}} = 65536$ and $N_G = 2 \times 10^6$ using our new scheme more than seven times faster than the direct scheme.

5.2. Comparison with Tree-based Algorithms

In previous studies, several tree-based algorithm with block timesteps were developed. Hernquist & Katz (1989) adopted block timesteps in a tree code. In their scheme, the tree is reconstructed in each step. When the timesteps of particle do not vary so widely, the cost of the tree reconstruction is not so expensive. However, the cost is very expensive for star clusters, because star clusters have wide range in their timesteps.

McMillan & Aarseth (1993) developed a tree-based high-order integration scheme for collisional systems using block timesteps and multipole (up to octupole) expansion. In this scheme, the tree is reconstructed at the appropriate cell timesteps determined by the motions of the particles in the cells. Instead of reconstructing tree at each step, the moment of each cell is predicted. However, the accuracy is limited by the time interval of tree construction. If longer timesteps are permitted, the tree evolves during the step and the errors increase. If the time interval is short, the cost of tree construction become large. In addition, their algorithms are difficult to use with GRAPE.

5.3. Applications to Other Problems

Our initial motivation for developing the Bridge scheme is to use it for the problem of a star cluster orbiting in its parent galaxy. However, it might have much wide application range. For example, if the parent galaxy has the central massive black hole, it is natural to handle it and stars near by with the direct scheme, and the rest of the system by tree. In this case, some particles must move “tree” and “direct” treatment, but in principle such a code can be developed. Our method can be applied to any large- N systems in which small part of the system shows collisional behavior.

The authors thanks Piet Hut for useful comments and the name of the hybrid scheme, Keigo Nitadori and Ataru Tanikawa for fruitful discussions, and the referee,

Simon F. Portegies Zwart, for useful comments on the manuscript. M. F. is financially supported by Research Fellowships of the Japan Society for the Promotion of Science (JSPS) for Young Scientists. This research is partially supported by the Special Coordination Fund for Promoting Science and Technology (GRAPE-DR project), Ministry of Education, Culture, Sports, Science and Technology, Japan. Part of calculations were done using the GRAPE system at the Center for Computational Astrophysics (CfCA) of the National Astronomical Observatory of Japan.

References

- Barnes, J., & Hut, P. 1986, *Nature*, 324, 446
 Casertano, S. & Hut, P. 1985, *ApJ* 298, 80
 Chandrasekhar, S. 1943, *ApJ*, 97, 255
 Cohn, H. 1980, *ApJ*, 242, 765
 Figer, D. F. 2004, in ASP Conf. Ser. 322, *The Formation and Evolution of Massive Young Star Clusters* (San Francisco: Astronomical Society of the Pacific), ed. H.J.G.L.M. Lamers, L.J. Smith, and A. Nota, & A. Nota, 49, astro-ph/0403088
 Fujii, M., Funato, Y., & Makino, J. 2006, *PASJ*, 58, 743
 Fukushige, T., Makino, J., & Kawai, A. 2005, *PASJ*, 57, 1009
 Gerhard, O. 2001, *ApJ*, 546, L39
 Ghez, A. M., et al. 2003, *ApJ*, 586, L127
 Gürkan, M. A., & Rasio, F. A. 2005, *ApJ*, 628, 236
 Hashimoto, Y., Funato, Y., & Makino, J. 2003, *ApJ*, 582, 196
 Heggie, D.C., & Mathieu, R.D. 1986, in *The Use of Supercomputers in Stellar Dynamics*, ed. P. Hut, and S. McMillan (Lecture Notes in Physics 267; Berlin: Springer), 233
 Hernquist, L. & Katz, N. 1989, *ApJS*, 70, 419
 Kim, S. S. & Morris, M. 2003, *ApJ*, 597, 312
 Kinoshita, H., Yoshida, H., & Nakai, H. 1991, *Celest. Mech. and Dyn. Astr.*, 50, 59
 Krabbe, A. et al. 1995, *ApJ*, 447, L95
 Levin, Y. & Beloborodov, A. M. 2003, *ApJ*, 590, L33
 Lu, J. R., Ghez, A. M., Hornstein, S. D., Morris, M., Thompson, D. J., & Becklin, E. E. 2006, *JPhCS*, 54, 279
 Makino, J. 1991, *PASJ*, 43, 621
 Makino, J. & Aarseth, S. J. 1992, *PASJ*, 44, 141
 Makino, J., Fukushige, T., Koga, M. & Namura, K. 2003, *PASJ*, 55, 1163
 Makino, J. 2004, *PASJ*, 56, 521
 McMillan, S. L. W. & Aarseth, S. J. 1993, *ApJ*, 414, 200
 Nagata, T., Woodward, E. C., Shure, M., & Kobayashi, N. 1995, *AJ*, 109, 1676
 Paumard, T., Maillard, J. P., Morris, M., & Rigaut, F. 2001 *A&A*, 366, 466
 Paumard, T. et al. 2006 *ApJ*, 643, 1011
 Portegies Zwart, S. F. & McMillan, S. L. W. 2002, *ApJ*, 576, 899
 Portegies Zwart, S. F., McMillan, S. L. W., & Gerhard, O. 2003, *ApJ*, 593, 352
 Spinnato, P. F., Fellhauer, M., & Portegies Zwart, S. F. 2003, *MNRAS*, 344, 22
 Spitzer, L. J. & Hart, M. H. 1971, *ApJ*, 164, 399
 Wisdom, J. & Holman, M. 1991, *AJ*, 102, 1528